Glycolaldehyde induces sensory neuron death through activation of the c-Jun N-terminal kinase and p-38 MAP kinase pathways

Tomoyo Akamine[1,2], Shizuka Takaku[1], Mari Suzuki[1], Naoko Niimi[1], Hideji Yako[1], Keiichiro Matoba[2], Daiji Kawanami[4], Kazunori Utsunomiya[3], Rimei Nishimura[2], Kazunori Sango[1]

[1]Diabetic Neuropathy Project, Department of Sensory and Motor Systems, Tokyo Metropolitan Institute of Medical Science, Setagaya-ku, Tokyo 156-8506, Japan

[2]Division of Diabetes, Metabolism & Endocrinology, Department of Internal Medicine, and [3]Center for Preventive Medicine, The Jikei University School of Medicine, Minato-ku, Tokyo 105-8461, Japan

[4]Department of Endocrinology and Diabetes Mellitus, Fukuoka University School of Medicine, Jonan-ku, Fukuoka 814-0180, Japan

Manuscript type: Short Communications

Number of characters in the text (not including Materials and Methods): 11,265

(Abstract; 1,089, Introduction; 3,044, Results & Discussion; 7,132)

Number of words in Abstract: 188

Number of Keywords: 6

Number of Figures: 4 (no supplementary figures)

Running head: Glycolaldehyde-induced sensory neuron death

Corresponding author

Kazunori Sango, M.D., Ph.D.

Diabetic Neuropathy Project, Department of Sensory and Motor Systems, Tokyo

Metropolitan Institute of Medical Science, 2-1-6 Kamikitazawa, Setagaya-ku, Tokyo 156-8506, Japan
TEL: 81-3-6834-2359
FAX: 81-3-5316-3150
E-mail: sango-kz@igakuken.or.jp

Abbreviations

AGEs, advanced glycation endproducts; 3-DG, 3-deoxyglucosone; DRG, dorsal root ganglia; ER, endoplasmic reticulum; GA, glycolaldehyde; GLA, glyceraldehyde; GO, glyoxal; IFRS1, immortalized adult Fischer rat Schwann cell 1; JNK, c-Jun N-terminal kinase; MAPK, mitogen activated kinase; MG, methylglyoxal; PNS, peripheral nervous system.

ABSTRACT

Glycolaldehyde (GA) is a highly reactive hydroxyaldehyde and one of the glycolytic metabolites producing advanced glycation endproducts (AGEs), but its toxicity toward neurons and Schwann cells remains unclear. In the present study, we found that GA exhibited more potent toxicity than other AGE precursors (glyceraldehyde, glyoxal, methylglyoxal and 3-deoxyglucosone) against immortalized IFRS1 adult rat Schwann cells and ND7/23 neuroblastoma × neonatal rat dorsal root ganglion (DRG) neuron hybrid cells. GA affected adult rat DRG neurons and ND7/23 cells more severely than GA-derived AGEs, and exhibited concentration- and time-dependent toxicity toward ND7/23 cells (10 < 100 < 250 < 500 μM; 6 h < 24 h). Treatment with 500 μM GA significantly up-regulated the phosphorylation of c-jun N-terminal kinase (JNK) and p-38 mitogen activated kinase (p-38 MAPK) in ND7/23 cells. Further, GA-induced ND7/23 cell death was significantly inhibited due to co-treatment with 10 μM of the JNK inhibitor SP600125 or the p-38 MAPK inhibitor SB239063. These findings suggest the involvement of JNK and p-38 MAPK signaling pathways in GA-induced neuronal cell death, and that enhanced GA production under diabetic conditions might be involved in the pathogenesis of diabetic neuropathy.

KEYWORDS

Diabetic neuropathy; Sensory neurons; Schwann cells; Viability; Glycolytic metabolites; Mitogen activated protein kinase signaling.

INTRODUCTION

Diabetic peripheral neuropathy (DPN), one of the most common complications of diabetes mellitus, severely affects patient's quality of life. Although the pathogenesis of DPN remains obscure, impaired insulin actions and subsequent hyperglycemia and dyslipidemia appear to play a major role in metabolic and vascular abnormalities in the peripheral nervous system (PNS) (Grisold et al., 2017). Under long-term hyperglycemic conditions, saturation of the glycolytic pathway and augmentation of the polyol and other collateral glucose-utilizing pathways accelerate the formation of advanced glycation endproducts (AGEs) and free-radicals, diminish the levels of nitric oxide and taurine, and alter the protein kinase C activity. These changes appear to be harmful to PNS constituents, especially neurons, Schwann cells, and blood vessels (Yagihashi, 2016).

AGEs are produced exogenously and endogenously via non-enzymatic reactions of amino acids/proteins and glucose or glycolytic metabolites such as glycolaldehyde (GA), glyceraldehyde (GLA), glyoxal (GO), methylglyoxal (MG), 3-deoxyglucosone (3-DG), and fructose (Takeuchi et al., 2015). Daily injection of AGEs into normal rats for 12 weeks resulted in increased serum AGE levels and reduced motor nerve conduction velocity, and nerve Na^+-K^+-ATPase activity (Nishizawa et al., 2010). Cytotoxic activity of AGEs against cultured neurons (Cellek et al., 2004), Schwann cells (Sekido et al., 2004), and microvascular endothelial cells (Shimizu et al., 2011) have also been reported. These findings suggest that production and accumulation of AGEs is one of the principal contributors to DPN. In addition to AGEs, their precursors, mainly MG and 3-DG, have been shown to impair the viability and function of neurons, Schwann cells, and endothelial cells (Suzuki et al., 1998; Kikuchi et al., 1999; Fukunaga et al., 2004; Ota et al., 2007; Tsukamoto et al., 2015; Navarrete Santos et al., 2017). It is noteworthy that increases in plasma MG level under diabetic conditions can evoke depolarization of nociceptive neurons, thereby causing hyperalgesia in DPN

(Bierhaus et al., 2012). In contrast to a considerable number of studies regarding the neurotoxic effects of MG and 3-DG, much less attention has been given to GA, a reactive α-hydroxyaldehyde. A single intravenous administration of GA was found to reduce anti-oxidant enzyme activity and enhance lipoperoxidation and protein carbonylation in kidneys, heart and liver of normal rats (Lorenzi et al., 2010a; 2010b; 2011). In addition, GA has been found to increase apoptosis in human breast cancer cells through inactivation of glycolytic and anti-oxidant enzymes (Al-Maghrebi et al., 2003), and increased cell death and protein carbonylation in rat hepatocytes (Yang et al., 2011). However, no studies addressed GA neurotoxicity until Sato et al. suggested the involvement of multidrug-resistance-associated protein (MRP-1) and endoplasmic reticulum (ER) stress in GA-induced injury and death of primary cultured Schwann cells (Sato et al., 2013; Sato et al., 2015). Schönhofen et al. briefly reported GA-induced death of SH-SY5Y human neuroblastoma cells (Schönhofen et al., 2015), but the underlying mechanisms remain unclear.

In the present study, we found that GA exhibited more potent cytotoxicity than other AGE precursors and GA-derived AGEs toward cultured neurons and Schwann cells, and that c-jun N-terminal kinase (JNK) and p-38 mitogen activated kinase (p-38 MAPK) signaling pathways are involved in GA-induced neuronal cell injury and death.

MATERIALS AND METHODS

Materials

Three-month-old female Wistar rats were purchased from CLEA Japan, Inc. (Shizuoka, Japan). Isofluorane was from Abbott Japan (Tokyo, Japan), Dulbecco's Modified Eagle's medium (DMEM), fetal bovine serum (FBS), and serum-free B27 supplement were from Thermo Fisher Scientific Inc. (Waltham, MA, USA). Collagenase Class III was from Worthington Biochemicals (Freehold, NJ, USA). GA, GLA, MG, trypsin, poly-L-lysine (PL) and anti-β-actin antibody [A5316] were purchased from

Sigma-Aldrich Co. LLC. (St. Louis, MO, USA). GO was from Nakalai Tesque Inc. (Kyoto, Japan), 3-DG was from Toronto Research Chemicals Inc. (North York, Canada), and GA-bovine serum albumin (GA-BSA) was from Cosmo Bio Co., LTD. (Tokyo, Japan). Percoll and the ECL plus Western blotting detection kit were from GE Healthcare Bio-Sciences Corp. (Piscataway, NJ, USA). The c- JNK inhibitor SP600125 and the p-38 mitogen activated protein kinase (MAPK) inhibitor SB239063 were from Calbiochem (La Jolla, CA, USA). Anti-JNK antibody [9252], anti-phospho-JNK antibody (Thr183/Tyr185) [4668], anti-p-38 MAPK antibody [8690], and anti-phospho-p-38 MAPK antibody (Thr180/Tyr182) [4511] were from Cell Signaling Technology (Beverly, MA, USA). Horseradish peroxidase (HRP)-conjugated anti-rabbit IgG and anti-mouse IgG antibodies were from Medical & Biological Laboratories Corp., Ltd. (Nagoya, Japan).

Cell culture

Dissociated cell culture of adult rat dorsal root ganglion (DRG) neurons was performed as previously described (Tsukamoto et al., 2015a). All the experiments were conducted in accordance with the Guidelines for the Care and Use of Animals of Tokyo Metropolitan Institute of Medical Science (2011). Prior to the dissection, rats were anesthetized for euthanasia with 3% isofluorane for 3 min (Niimi et al., 2018). DRGs from the cervical to the lumbar level were dissected from each animal, incubated at 37°C with 0.2% collagenase for 2 h and 0.25% trypsin for 15 min, and then subjected to density gradient centrifugation (5 min, 200 g) with 30% Percoll to eliminate the myelin sheaths. This procedure resulted in a yield of $> 5 \times 10^4$ neurons with a small number of non-neuronal cells. The neurons were suspended in DMEM supplemented with 10% FBS, and seeded on PL (10 μg/mL)-coated wells of 12-well culture plates. Circles with a diameter of 0.9 cm were delineated using black thin lines on the bottom of each well, and the neuronal cell density was adjusted to approximately 500–600 cells within the

144 circle.

145 Spontaneously immortalized Schwann cells IFRS1 from adult Fischer 344 rats
146 (Sango et al., 2011) at the 30–40 passage state and ND7/23 mouse neuroblastoma/rat
147 embryonic DRG neuron hybrid cells (Wood et al., 1990) at the 15–25 passage state
148 were maintained in DMEM supplemented with 5% FBS, and employed for the
149 following assays.

150

151 *Cell viability assays*

152 After dissociation and overnight incubation in the serum-containing medium,
153 DRG neurons were maintained for 48 h in DMEM supplemented with B27 in the
154 presence or absence of 500 μM GA or GA-BSA. Dead neurons were detected using
155 positive trypan blue staining, and the number of viable (trypan blue-negative) neurons
156 within the specified area in each well was counted under a phase-contrast light
157 microscope. The cell viability ratio was calculated as the number of viable neurons /
158 total neurons within the specified area in each well, and normalized to the percentage of
159 the average viable neurons in the control (DMEM/B27 with no additive).

160 The toxicity of AGE precursors (GA, GLA, MG, 3-DG and GO) and GA-BSA
161 toward ND7/23 and IFRS1 cells was evaluated by using the CellTiter 96® AQueous One
162 Solution Cell Proliferation Assay kit (Promega, Madison, WI, USA) following the
163 manufacturer's instructions. The cells were seeded in each well of 96-well culture plates
164 at an approximate density of $3 \times 10^4/cm^2$, and incubated in DMEM supplemented with
165 5% FBS for 16 h. The cells were then maintained in DMEM supplemented with 1%
166 FBS in the presence or absence of each AGE precursor or GA-BSA for 6–48 h. After
167 rinsing with 250 μL FBS-free DMEM, the cells were incubated for 1–2 h at 37°C in 100
168 μL of FBS-free DMEM with 10 μL of CellTiter 96® AQueous One Solution Reagent.
169 Absorbance at 490 nm was determined with a plate reader (Varioskan Flash; Thermo
170 Scientific), and cell viability in each culture condition was expressed as the percentage

171 of the absorbance in the control condition (DMEM/1% FBS with no additive)
172 (Tsukamoto et al., 2015b).
173
174 *Western blotting*
175 ND7/23 cells at semi-confluency in 100 mm culture plates were incubated in
176 DMEM supplemented with 1%FBS in the presence or absence of 500 μM GA for 1 h.
177 The cells were lysed with 1× sodium dodecyl sulfate (SDS) sample buffer.
178 SDS-polyacrylamide gel electrophoresis (SDS-PAGE) was performed using 5–20%
179 SDS-PAGE gel (FUJIFILM, Tokyo, Japan). After electrophoresis, the proteins were
180 transferred onto a PVDF membrane using an electroblotter (Nihon Eido Co., Ltd.,
181 Tokyo, Japan). The membrane was incubated in PBS with 0.1% Tween 20 (including
182 5% skimmed milk or 3% BSA) for 1 h at room temperature, and then overnight at 4°C
183 with anti-JNK antibody (1:1000), anti-phospho-JNK antibody (1:1000), anti-p38
184 MAPK antibody (1:1000), anti-phospho-p38 MAPK antibody (1:1000), or anti-β-actin
185 antibody (1:3000). After rinsing with PBS containing 0.1% Tween 20, the membranes
186 were incubated in a solution of HRP-conjugated secondary anti-rabbit IgG antibody or
187 anti-mouse IgG antibody (1:2000) for 1 h. After washing, immunocomplexes on the
188 membrane were visualized with the ECL plus Western blotting detection kit. The signal
189 intensity was quantified using an Ez-Capture II chemiluminescence imaging system
190 (Atto Corp., Tokyo, Japan), and the relative signal intensity of each protein was
191 expressed as the intensity of each protein / intensity of β-actin. The specificity of the
192 primary antibodies used in the blotting is documented in the following web sites and
193 articles;
194 anti-JNK antibody;
195 https://en.cellsignal.jp/products/primary-antibodies/sapk-jnk-antibody/9252 (Neganova
196 et al., 2016),
197 anti-phospho-JNK antibody;

https://en.cellsignal.jp/products/primary-antibodies/phospho-sapk-jnk-thr183-tyr185-81e11-rabbit-mab/4668 (Bose & Janes 2013),
anti-p38 MAPK antibody;
https://en.cellsignal.jp/products/primary-antibodies/p38-mapk-d13e1-xp-rabbit-mab/8690 (Li et al., 2017),
anti-phospho-p38 MAPK antibody;
https://en.cellsignal.jp/products/primary-antibodies/phospho-p38-mapk-thr180-tyr182-d3f9-xp-rabbit-mab/4511 (Bose & Janes 2013), and
anti-β-actin antibody:
https://www.sigmaaldrich.com/catalog/product/sigma/a5316?lang=en&region=US
(North et al., 1994).

Statistical analysis

All the data are expressed as means and standard errors (SEM), and the number of experiments is indicated in the figure legends. Statistical comparison between two groups was performed using two-tailed Student's t-test. Data involving more than two groups were assessed using ANOVA followed by Bonferroni's post hoc correction. Statistical analyses were conducted using Ekuseru-Toukei 2010 (Social Survey Research Information Co., Ltd., Tokyo, Japan). A normal distribution was assumed for all experimental groups. A value of $P < 0.05$ was considered as statistically significant.

RESULTS & DISCUSSION

Formation of AGEs from glucose and glycolytic metabolites including GA is associated with the development of DPN and other diabetic complications (Brings et al., 2017), as well as Alzheimer's disease (AD) and other neurodegenerative disorders (Pugazhenthi et al., 2017). Several articles addressed the neurotoxic effects of GA-derived AGEs (Luo et al., 2002; Takeuchi et al., 2000; Choei et al., 2004; Bikbova

et al., 2013), and the toxicity may be attributable, at least partly, to the AGE–receptor for AGEs (RAGE) axis that triggers intracellular signaling pathways associated with inflammation and oxidative stress (Yamagishi et al., 2002; Nam et al., 2015). In contrast, GA *per se* has not drawn attention as a cause of DPN or AD and it was only recently that deleterious effects of GA on SH-SY5Y neuroblastoma cells (Schönhofen et al., 2015) and primary cultured Schwann cells (Sato et al., 2013; Sato et al., 2015) were documented; these reports, especially the latter, suggested possible involvement of GA in the pathogenesis of DPN and inspired the present study.

We found that under the same concentration (500 μM) and exposure time (24 h), GA, MG, and GO significantly reduced the viability ratios as compared with control in both IFRS1 and ND7/23 cells; GLA significantly reduced the viability of ND7/23 cells, but not IFRS1 cells, whereas no apparent IFRS1 or ND7/23 cell death was induced due to exposure to 3-DG. Thus, GA was found to be more harmful than other metabolites (3-DG, MG, GLA, and GO) against IFRS1 and ND7/23 cells (**Fig. 1**). In agreement with these findings, significant cell death of primary cultured Schwann cells was induced due to a 24-h exposure to 500 μM GA, but not 3-DG, MG, or GO (Sato et al., 2013).

Because the detrimental effects of GA on Schwann cells have already been documented (Sato et al., 2013; Sato et al., 2015), the following experiments were conducted with a focus on the mechanisms of GA-induced neuronal cell injury and death. Treatment with 500 μM GA for 24–48 h significantly reduced the viability ratios of primary cultured DRG neurons and ND7/23 cells compared with control, whereas GA-derived AGEs (GA-BSA) at the same concentration had less potent toxicity than GA against the both the neuronal cell types (**Fig. 2a, b**). Moreover, GA toxicity against ND7/23 cells was concentration-dependent (10 < 100 < 250 < 500 μM) and time-dependent (6 h < 24 h) (**Fig. 2c**). Consistently, the toxicity of 10 mM GA against rat hepatocytes showed a time-dependency (1 h < 2 h < 3 h) (Yang et al., 2011),

252 whereas breast cancer cell death was induced by GA at 500 μM for 24 h, but not at 100
253 μM for 72 h (Al-Maghrebi et al., 2003). These findings suggest that GA cytotoxicity is
254 largely dependent on its concentration and exposure duration. GA-AGEs formed and
255 accumulated in GA-treated cells might be involved in mediating GA toxicity, but the
256 accumulation of GA-AGEs appears to require incubation of the cells with GA for longer
257 than 24 h (Yamabe et al., 2013). Because 6-h incubation with GA resulted in significant
258 ND7/23 cell death (**Fig. 2c**), reduced viability under exposure to GA appears more
259 attributable to direct GA toxicity rather than the formation of GA-AGEs. It is also
260 noteworthy that GA showed more potent toxicity than GA-AGEs (GA-BSA) toward
261 primary cultured DRG neurons and ND7/23 cells (**Figs. 2a, b**). Because GA-BSA has a
262 much higher molecular weight than GA, careful attention should be paid to the
263 comparisons between the two molecules at the same concentration (500 μM). In a
264 previous study (Sekido et al., 2004), treatment with GA-BSA for 24 h reduced the
265 viability of primary cultured Schwann cells in a concentration-dependent manner (10 <
266 500 < 1,000 μg/mL), but the average viability ratio at the highest concentration (1,000
267 μg/mL) was nearly 70% of control. In contrast, we and others (Sato et al., 2013)
268 observed that treatment with the maximum dose (500 μM ≈ 30 μg/mL) of GA for 24 h
269 diminished the viability of neurons and Schwann cells to a level approximately 40% of
270 control. These findings allow us to speculate that GA activates the injury signals from
271 inside and/or outside the cells more rapidly and effectively than GA-AGEs.
272 Several studies have indicated the involvement of MAP kinase (JNK, p-38 MAPK
273 and ERK) signaling pathways in apoptotic cell death of DRG neurons under exposure to
274 neurotoxic substances (Bodner et al., 2004; Scuteri et al., 2010; Agthong et al., 2012).
275 Western blot analysis showed that treatment with 500 μM GA for 1 h significantly
276 up-regulated phosphorylation of JNK (**Fig. 3a**) and p-38 MAPK (**Fig. 3b**). Consistent
277 with these findings, GA-induced ND7/23 cell death was significantly inhibited due to
278 co-treatment with 10 μM of the JNK inhibitor SP600125 or the p-38 MAPK inhibitor

279 SB239063 (**Fig. 3c**). To our knowledge, no other studies have targeted the signaling
280 molecules and pathways mediating GA cytotoxicity. MAP kinases are key elements in
281 signal transduction machinery, and they play a major role in various kinds of reactions
282 associated with cell growth, differentiation and death (Johnson & Lapadat, 2002). The
283 involvement of MAP kinase signaling pathways in MG-mediated neurotoxicity has been
284 investigated; it induced neural progenitor cell death through ERK signaling activation
285 (Chun et al., 2016), Schwann cell death through JNK and p-38 MAPK activation
286 (Fukunaga et al., 2004; Ota et al., 2007), and increased inflammatory responses in
287 astrocytes through JNK activation (Chu et al., 2016). Because both GA and MG are
288 reactive aldehydes generated through the Maillard reaction, we speculated that there
289 might be some similarities in the neurotoxic actions between the two molecules, and
290 investigated MAP kinase signaling pathways in the present study. GA up-regulated the
291 phosphorylation of JNK and p-38 MAPK in ND7/23 cells (**Figs. 3a, b**), and the JNK
292 inhibitor SP600125 and the p-38 MAPK inhibitor SB239063 partially but significantly
293 alleviated GA-induced cell death (**Fig. 3c**). These findings suggest that both JNK and
294 p-38 MAPK signaling pathways play a pivotal role in GA-induced neuronal cell death.
295 The induction of these signals at 1 h after GA exposure supports our notion that GA
296 rapidly activates injury signals as described above. With regard to the apoptotic signals,
297 our immunofluorescence and western blot analyses revealed GA-induced up-regulation
298 of cleaved caspase-3 expression in ND7/23 cells (Akamine et al., personal
299 communication); however, possible relationship between caspase-3 and JNK or p-38
300 MAPK signaling pathways remain to be elucidated. It has been reported that ER stress
301 plays a major role in apoptosis of Schwann cells under GA exposure (Sato et al., 2015).
302 In our study, treatment with GA tended to up-regulate the expression of some molecules
303 involved in ER stress (*e.g.*, activation transcription factor 4 and C/EBP homologous
304 protein) in ND7/23 cells (Akamine et al., personal communication); however,
305 GA-induced ND7/23 cell death was not rescued due to co-treatment with

306 4-phenylbutyric acid, an ER stress inhibitor (**Fig. 3c**). Although further analyses are
307 needed, ER stress may not be crucial in GA-induced neuronal cell death.
308 In conclusion, the findings of the present study suggest the involvement of the
309 JNK and p-38 MAPK signaling pathways in GA-induced neuronal cell death. Our
310 ongoing investigation focuses on the signaling molecules downstream of JNK and p-38
311 MAPK, possible cross-talk between the two pathways, and precise cascades leading to
312 the neurotoxicity, *e.g.,* caspase-3 and other apoptotic signals, oxidative stress and
313 impaired energy production (Al-Maghrebi et al., 2003; Rodrigo Lorenzi et al., 2010)
314 (**Fig. 4**). It is also of critical significance to investigate the GA neurotoxicity using *in*
315 *vivo* systems. Because GA administration induced decreases in the activity of
316 anti-oxidant enzymes in kidneys, heart and liver of normal rats (Lorenzi et al., 2010a;
317 2010b; 2011), we plan to assess the oxidative damages of the peripheral nervous tissue
318 in rats under exposure to similar GA load. In addition, our preliminary study using DRG
319 neuron–IFRS1 Schwann cell co-culture system (Sango et al., 2011), which mimics *in*
320 *vivo* conditions better than single cell culture systems, revealed that GA induced axonal
321 degeneration- and demyelination-like changes (Akamine et al., personal
322 communication). Further studies with these systems may strengthen our hypothesis that
323 GA is involved in the pathogenesis of DPN.
324
325 **ACKNOWLEDGMENTS**
326 This study was supported by a Grant-in-aid for Scientific Research from the
327 Ministry of Education, Science, Sports and Culture of Japan (JSPS KAKENHI
328 16K07048). We would like to thank Prof. Atsufumi Kawabata and Dr. Fumiko
329 Sekiguchi (Laboratory of Pharmacology and Pathophysiology, Faculty of Pharmacy,
330 Kindai University, Higashi-Osaka, Japan) for providing us ND7/23 cells, and Prof.
331 Shuji Mori (Department of Pharmacology, School of Pharmacy, Shujitsu University,
332 Okayama, Japan) for helpful suggestions on AGEs preparation.

CONFLICT OF INTEREST STATEMENT

The authors declare no conflict of interest.

CONTRIBUTORS

T.A. designed and conducted the experiments, and wrote the manuscript. S.T., M.S., N.N., H.Y., K.M., D.K., K.U. and R.N. conducted the experiments and discussed the results. K.S. designed the experiments, wrote the manuscript and supervised the project.

REFERENCES

Agthong S, Kaewsema A, Chentanez V (2012) Inhibition of p38 MAPK reduces loss of primary sensory neurons after nerve transection. Neurol Res 34:714-720

Al-Maghrebi M, Al-Mulla F, Benov L (2003) Glycolaldehyde induces apoptosis in a human breast cancer cell line. Arch Biochem Biophys 417:123-127

Bierhaus A, Fleming T, Stoyanov S, Leffler A, Babes A, Neacsu C, K Sauer S, Mirjam Eberhardt M, Schnölzer M, Lasitschka F, L Neuhuber W, I Kichko T, Konrade I, Elvert R, Mier W, Pirags V, K Lukic I, Morcos M, Dehmer T, Rabbani N, J Thornalley P, Edelstein D, Nau C, Forbes J, M Humpert P, Schwaninger M, Ziegler D, M Stern D, E Cooper M, Haberkorn U, Brownlee M, W Reeh P & P Nawroth P (2012) Methylgloxal modification of Nav1.8 facilitates nociceptive neuron firing and causes hyperalgesia in diabetic neuropathy. Nat Med 18:926-933

Bikbova G, Oshitari T, Yamamoto S (2013) Neurite regeneration in adult rat retinas exposed to advanced glycation end-products and regenerative effects of neurotrophin-4. Brain Res 1534:33-45

Bodner A, Toth PT, Miller RJ (2004) Activation of c-Jun N-terminal kinase mediates gp120IIIB- and nucleoside analogue-induced sensory neuron toxicity. Exp Neurol 188:246-253

Bose AK, Janes KA (2013) A high-throughput assay for phosphoprotein-specific phosphatase activity in cellular extracts. Mol Cell Proteomics 12:797-806

Brings S, Fleming T, Freichel M, Muckenthaler M, Herzig S, Nawroth P (2017) Dicarbonyls and advanced glycation end-products in the development of diabetic complications and targets for intervention. Int J Mol Sci 18

Cellek S, Qu W, Schmidt AM, Moncada S (2004) Synergistic action of advanced glycation end products and endogenous nitric oxide leads to neuronal apoptosis in vitro: a new insight into selective nitrergic neuropathy in diabetes. Diabetologia 47:331-339

Choei H, Sasaki N, Takeuchi M, Yoshida T, Ukai W, Yamagishi S, Saito T (2004) Glyceraldehyde-derived advanced glycation end products in Alzheimer's disease. Acta Neuropathol 108:189-193

Chu JM, Lee DK, Wong DP, Wong GT, Yue KK (2016) Methylglyoxal-induced neuroinflammatory response in in vitro astrocytic cultures and hippocampus of experimental animals. Metab Brain Dis 31:1055-1064

Chun HJ, Lee Y, Kim AH, Lee J (2016) Methylglyoxal Causes Cell Death in Neural Progenitor Cells and Impairs Adult Hippocampal Neurogenesis. Neurotox Res 29:419-431

Fukunaga M, Miyata S, Liu B, Miyazaki H, Hirota Y, Higo S, Hamada Y, Ueyama S, Kasuga M (2004) Methylglyoxal induces apoptosis through activation of p38 MAPK in rat Schwann cells. Biochem Biophys Res Commun 320:689-695

Grisold A, Callaghan B, Feldman E (2017) Mediators of diabetic neuropathy – is hyperglycemia the only culprit? Curr Opin Endcrinol Diabetes Obes 24:103-111

396

397 Johnson GL & Lapadat R (2002) Mitogen-activated protein kinase pathways mediated
398 by ERK, JNK, and p38 protein kinases. Science 298:1911-1912

399

400 Kikuchi S, Shinpo K, Moriwaka F, Makita Z, Miyata T, Tashiro K (1998) Neurotoxicity
401 of methylgloxal and 3-deoxyglucosone on cultured cortical neurons: Synergism
402 between glycation and oxidative stress, possibly involved neurodegenerative diseases. J
403 Neurosci Res 57:280-289

404

405 Li W, Zhu J, Dou J, She H, Tao K, Xu H, Yang Q, Mao Z (2017) Phosphorylation of
406 LAMP2A by p38 MAPK couples ER stress to chaperone-mediated autophagy. Nat
407 Commun 8:1763

408

409 Lorenzi R, Andrades ME, Bortolin RC, Nagai R, Dal-Pizzol F, Moreira JC (2010a)
410 Circulating glycoaldehyde induces oxidative damage in the kidney of rats. Diabetes Res
411 Clin Pract 89:262-267

412

413 Lorenzi R, Andrades ME, Bortolin RC, Nagai R, Dal-Pizzol F, Moreira JC (2010b)
414 Glycolaldehyde induces oxidative stress in the heart: a clue to diabetic cardiomyopathy?
415 Cardiovasc Toxicol 10:244-249

416 Lorenzi R, Andrades ME, Bortolin RC, Nagai R, Dal-Pizzol F, Moreira JC (2011)
417 Oxidative damage in the liver of rats treated with glycolaldehyde. Int J Toxicol
418 30:253-258

419

420 Luo ZJ, King RH, Lewin J, Thomas PK (2002) Effects of nonenzymatic glycosylation

421 of extracellular matrix components on cell survival and sensory neurite extension in cell
422 culture. J Neurol 249:424-431
423
424 Nam MH, Son WR, Lee YS, Lee KW (2015) Glycolaldehyde-derived advanced
425 glycation end products (glycol-AGEs)-induced vascular smooth muscle cell dysfunction
426 is regulated by the AGES-receptor (RAGE) axis in endothelium. Cell Commun Adhes
427 22:67-78
428
429 Navarrete Santos A, Jacobs K, Simm A, Glaubitz N, Horstkorte R, Hofmann B (2017)
430 Dicarbonyls induce senescence of human vascular endothelial cells. Mech Ageing Dev
431 166:22-32
432
433 Neganova I, Shmeleva E, Munkley J, Chichagova V, Anyfantis G, Anderson R, Passos
434 J, Elliott DJ, Armstrong L, Lako M (2016) JNK/SAPK signaling is essential for
435 efficient reprogramming of human fibroblasts to induced pluripotent stem cells. Stem
436 Cells 34:1198-1212
437
438 Niimi N, Yako H, Takaku S, Kato H, Matsumoto T, Nishito Y, Watabe K, Ogasawara S,
439 Mizukami H, Yagihashi S, Chung SK, Sango K (2018) A spontaneously immortalized
440 Schwann cell line from aldose reductase-deficient mice as a useful tool for studying
441 polyol pathway and aldehyde metabolism. J Neurochem 144:710-722
442
443 Nishizawa Y, Wada R, Baba M, Takeuchi M, Hanyu-Itabashi C, Yagihashi S (2010)
444 Neuropathy induced by exogenously administered advanced glycation end-products in
445 rats. J Diabetes Investig 1:40-49
446

447 North AJ, Gimona M, Lando Z, Small JV (1994) Actin isoform compartments in
448 chicken gizzard smooth muscle cells. J Cell Sci 107:445-455

449

450 Ota K, Nakamura J, Li W, Kozakae M, Watarai A, Nakamura N, Yasuda Y, Nakashima
451 E, Naruse K, Watabe K, Kato K, Oiso Y, Hamada Y (2007) Metformin prevents
452 methylglyoxal-induced apoptosis of mouse Schwann cells. Biochem Biophys Res
453 Commun 357:270-275

454

455 Pugazhenthi S, Qin L, Reddy PH (2017) Common neurodegenerative pathways in
456 obesity, diabetes, and Alzheimer's disease. Biochim Biophys Acta 1863:1037-1045

457

458 Sango K, Yanagisawa H, Kawakami E, Takaku S, Ajiki K, Watabe K (2011)
459 Spontaneously immortalized Schwann cells from adult Fischer rat as a valuable tool for
460 exploring neuron-Schwann cell interactions. J Neurosci Res 89:898-908

461

462 Sato K, Tatsunami R, Yama K, Tampo Y (2013) Glycolaldehyde induces cytotoxicity
463 and increases glutathione and multidrug-resistance-associated protein levels in Schwann
464 cells. Biol Pharm Bull 36:1111-1117

465

466 Sato K, Tatsunami R, Yama K, Tampo Y (2015) Glycolaldehyde induces endoplasmic
467 reticulum stress and apoptosis in Schwann cells. Toxicol Rep 2:1454-1462

468

469 Schönhofen P, de Meiros LM, Bristot IJ, Lopes FM, De Bastiani MA, Kapczinski F,
470 Crippa JA, Castro MA, Parsons RB, Klame F (2015) Cannabidiol exposure during
471 neuronal differentiation sensitizes cells against redox-active neurotoxins. Mol Neurobiol
472 52:26-37

Scuteri A, Galimberti A, Ravasi M, Pasini S, Donzelli E, Cavaletti G, Tredici G (2010) NGF protects dorsal root ganglion neurons from oxaliplatin by modulating JNK/Sapk and ERK1/2. Neurosci Lett 486:141-145

Sekido H, Suzuki T, Jomori T, Takeuchi M, Yabe-Nishimura C, Yagihashi S (2004) Reduced cell replication and induction of apoptosis by advanced glycation end products in rat Schwann cells. Biochem and Biophys Res Comm 320:241-248

Shimizu F, Sano Y, Haruki H, Kanda T (2011) Advanced glycation end-products induce basement membrane hypertrophy in endoneurial microvessels and disrupt the blood-nerve barrier by stimulating the release of TGF-β and vascular endothelial growth factor (VEGF) by pericytes. Diabetologia 54:1517-1526

Suzuki K, Ho Koh Y, Mizuno H, Hamaoka R, Taniguchi N (1998) Overexpression of aldehyde reductase protects PC12 cells from the cytotoxicity of methylglyoxal or 3-deoxyglucosone. J Biochem 123:353-357

Takeuchi M, Bucala R, Suzuki T, Ohkubo T, Yamazaki M, Koike T, Kameda Y, Makita Z (2000) Neurotoxicity of advanced glycation end-products for cultured cortical neurons. J Neuropathol Exp Neurol 59:1094-1105

Takeuchi M, Takino J, Furuno S, Shirai H, Kawakami M, Muramatsu M, Kobayashi Y, Yamagishi S (2015) Assessment of the concentrations of various advanced glycation end-products in beverages and foods that are commonly consumed in Japan. PLoS One 10:e0118652

Tsukamoto M, Niimi N, Sango K, Takaku S, Kanazawa Y, Utsunomiya K (2015a) Neurotrophic and neuroprotective properties of exendin-4 in adult rat dorsal root ganglion neurons: involvement of insulin and RhoA. Histochem Cell Biol 144:249-259

Tsukamoto M, Sango K, Yanagisawa H, Watabe K, Utsunomiya K (2015b) Upregulation of galectin-3 in immortalized Schwann cells IFRS1 under diabetic conditions. Neurosci Res 92:80-85

Wood JN, Bevan SJ, Coote PR, Dunn PM, Harmar A, Hogan P, Latchman DS, Morrison C, Rougon G, Theveniau M, Wheatley S (1990) Novel cell lines display properties of nociceptive sensory neurons. Proc Biol Sci 241:187-194

Yagihashi S (2016) Glucotoxic mechanisms and related therapeutic approaches. Int Rev Neurobiol 127:121-149

Yamabe S, Hirose J, Uehara Y, Okada T, Okamoto N, Oka K, Taniwaki T, Mizuta H (2013) Intracellular accumulation of advanced glycation end products induces apoptosis via endoplasmic reticulum stress in chondrocytes. FEBS J 280:1617-1629

Yamagishi S, Amano S, Inagaki Y, Okamoto T, Koga K, Sasaki N, Yamamoto H, Takeuchi M, Makita Z (2002) Advanced glycation end products-induced apoptosis and overexpression of vascular endothelial growth factor in bovine retinal pericytes. Biochem Biophys Res Commun 290:973-978

Yang K, Feng C, Lip H, Bruce WR, O'Brien PJ (2011) Cytotoxic molecular mechanisms and cytoprotection by enzymic metabolism or autoxidation for glyceraldehyde, hydroxypyruvate and glycolaldehyde. Chem Biol Interact 191:315-321

527

FIGURE LEGENDS

Figure 1. The viability of IFRS1 cells (**upper**) and ND7/23 cells (**lower**) after 24 h exposure to 500 μM of each precursor of AGEs (GA, 3-DG, MG, GLA, or GO); MTS assay. The optimal density at 490 nm in each well was measured with a plate reader, and normalized to the percentage of the value at control (DMEM/1% FBS). Data are expressed as means ± SEM of six experiments (individual values are depicted as circles, squares, and triangles); **P < 0.01 as compared with control.

Figure 2. GA showed more potent toxicity than GA-BSA toward cultured adult rat DRG neurons and ND7/23 cells. (**a**) Representative phase-contrast micrographs of DRG neurons (**upper**) and ND7/23 cells (**lower**) after exposure to 500 μM GA or GA-BSA. Dead cells were detected using positive trypan blue staining. (**b**) The viability ratio of DRG neurons after 48 h expose to 500 μM GA or GA-BSA (**left**) was calculated as the number of viable (trypan blue-negative) neurons / total neurons within the specified area in each well, and normalized to the percentage of the average viable neurons in control. Data are expressed as means ± SEM of six experiments; **P < 0.01 as compared with control. The viability of ND7/23 cells after 24-h expose to 500 μM GA or GA-BSA (**right**) was determined using MTS assay, and normalized to the percentage of the value in control. Data are expressed as means ± SEM of three experiments; *P < 0.05 and **P < 0.01 as compared with control. (**c**) GA induced ND7/23 cell death in a dose-dependent manner (10 < 100 < 250 < 500 μM). The cell viability after 6-h (**left**) or 24-h (**right**) exposure to GA was determined using MTS assay, and normalized to the percentage of the value in control. Data are expressed as means ± SEM of six experiments; *P < 0.05 and **P < 0.01 as compared with control.

Figure 3. Treatment of ND7/23 cells with 500 μM GA for 1 h induced phosphorylation

555 of JNK (**a**) and p38 MAPK (**b**); Western blot analysis. The representative picture of the
556 blot (**upper**) and quantitative data (**lower**) are shown. Data are expressed as means ±
557 SEM of three experiments; **P < 0.01 as compared with control. (**c**) GA-induced
558 ND7/23 cell death was ameliorated due to co-treatment with the JNK inhibitor
559 SP600125 and the p38 MAPK inhibitor SB239063, but not with the ER stress inhibitor
560 4-PBA. The viability of ND7/23 cells after 8-h expose to 500 μM GA in the presence or
561 absence of 10 μM SP600125 (**SP**), 10 μM SB239063 (**SB**), or 1mM 4-PBA was
562 determined using MTS assay, and normalized to the percentage of the value in control.
563 Data are expressed as means ± SEM of six experiments; **P < 0.01 as compared with
564 GA with no additive.
565
566 **Figure 4**. Schematic diagram showing the mechanisms of GA-induced neuronal cell
567 death based on the present study and possible relationship between the signaling
568 pathways and pathogenic factors suggested by the previous and present studies. ROS;
569 reactive oxygen species.

Figure 1

(a)

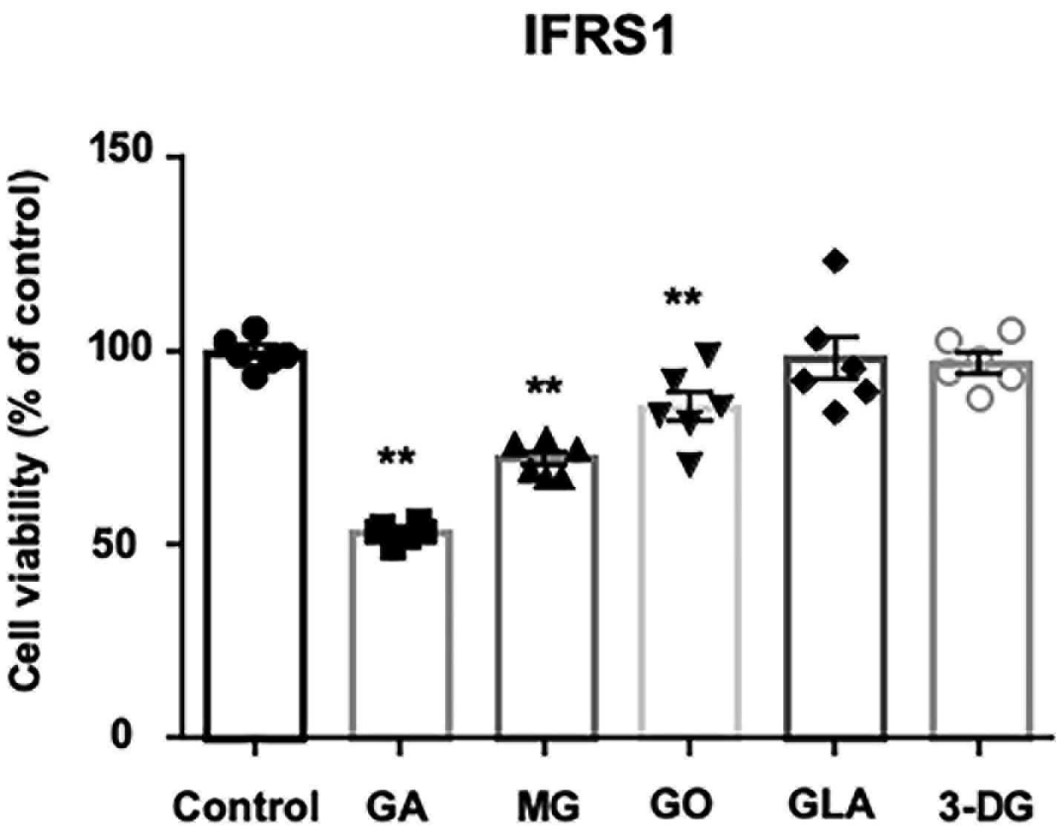
IFRS1
Cell viability (% of control)
150
100
50
0
**
**
**
Control
GA
MG
GO
GLA
3-DG

(b)

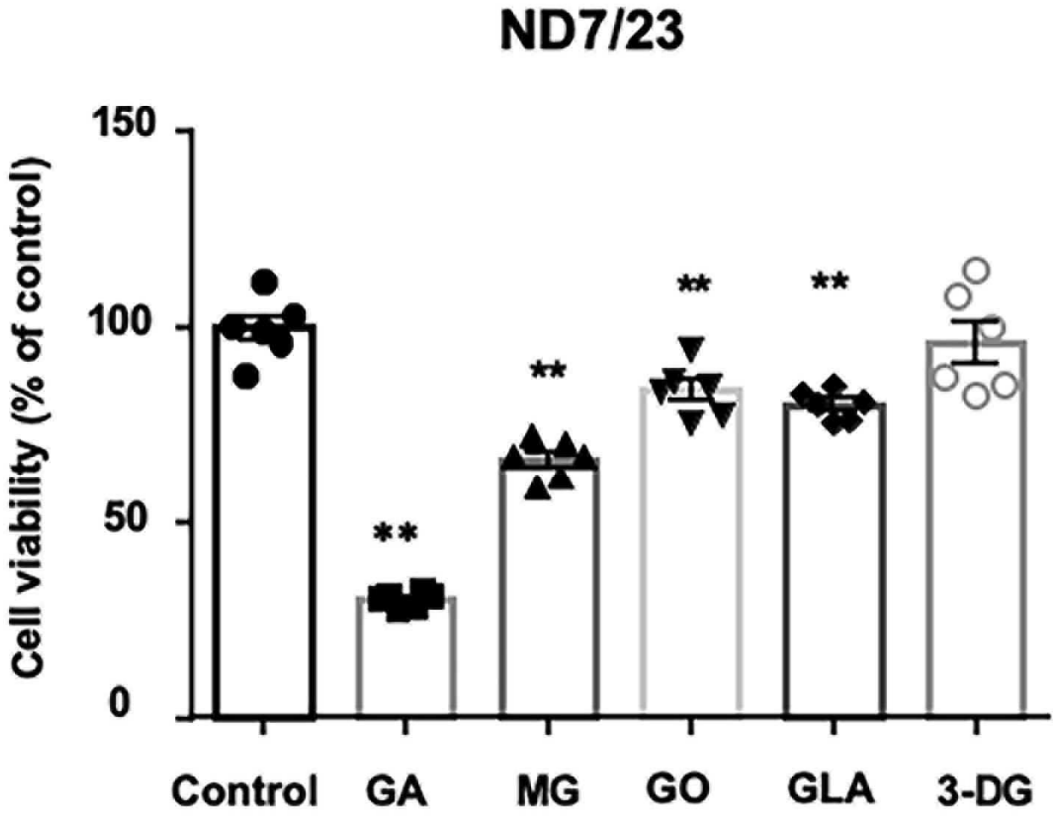
ND7/23
Cell viability (% of control)
150
100
50
0
**
**
**
**
Control
GA
MG
GO
GLA
3-DG

Figure 2

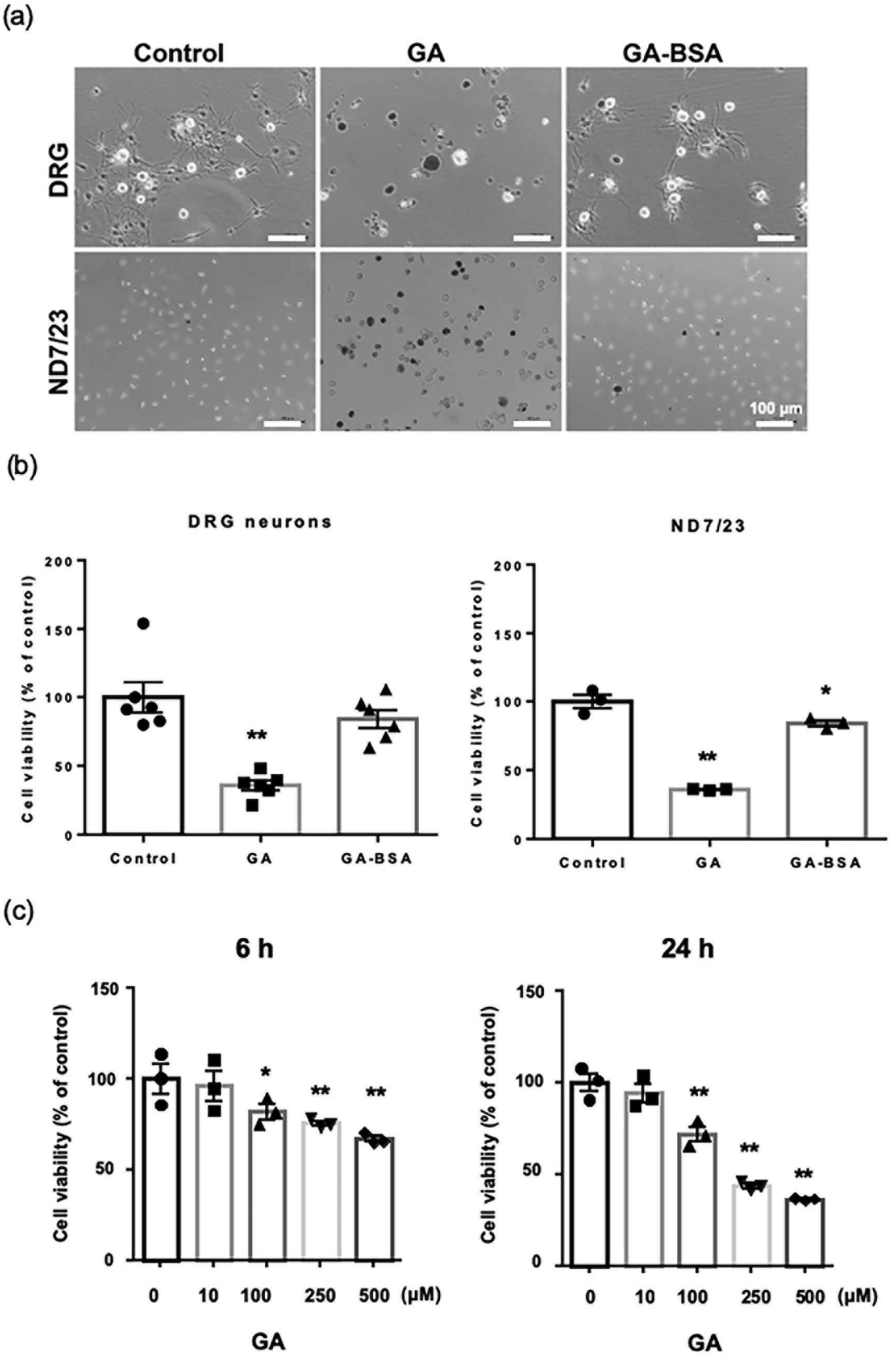
(a)
Control
GA
GA-BSA
DRG
ND7/23
100 μm
(b)
DRG neurons
ND7/23
Cell viability (% of control)
200
150
100
50
0
**
*
Control
GA
GA-BSA
(c)
6 h
24 h
Cell viability (% of control)
150
100
50
0
*
**
0
10
100
250
500
(μM)
GA

Figure 3

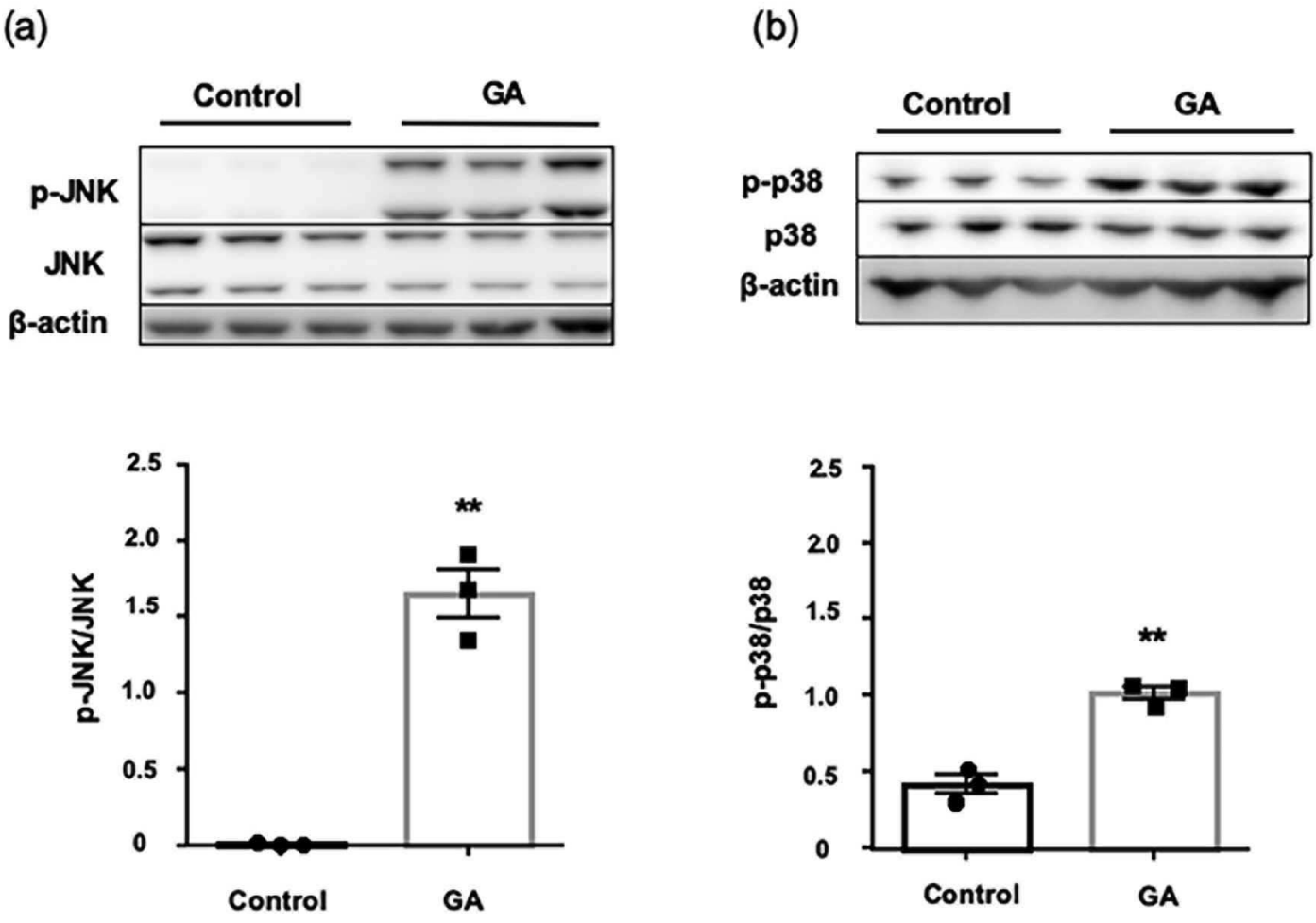
(a)
Control
GA
p-JNK
JNK
β-actin
p-JNK/JNK
2.5
2.0
1.5
1.0
0.5
0
**
Control
GA
(b)
Control
GA
p-p38
p38
β-actin
p-p38/p38
2.5
2.0
1.5
1.0
0.5
0
**
Control
GA

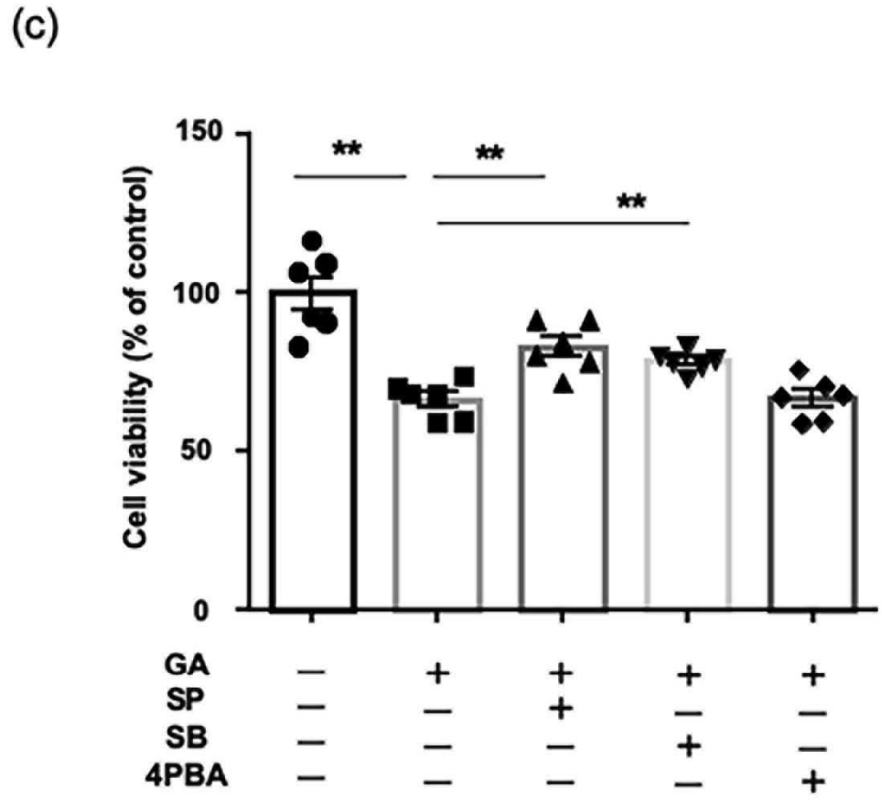
(c)
Cell viability (% of control)
150
100
50
0
**
**
**
GA
SP
SB
4PBA
— + + + +
— — + — —
— — — + —
— — — — +

Figure 4

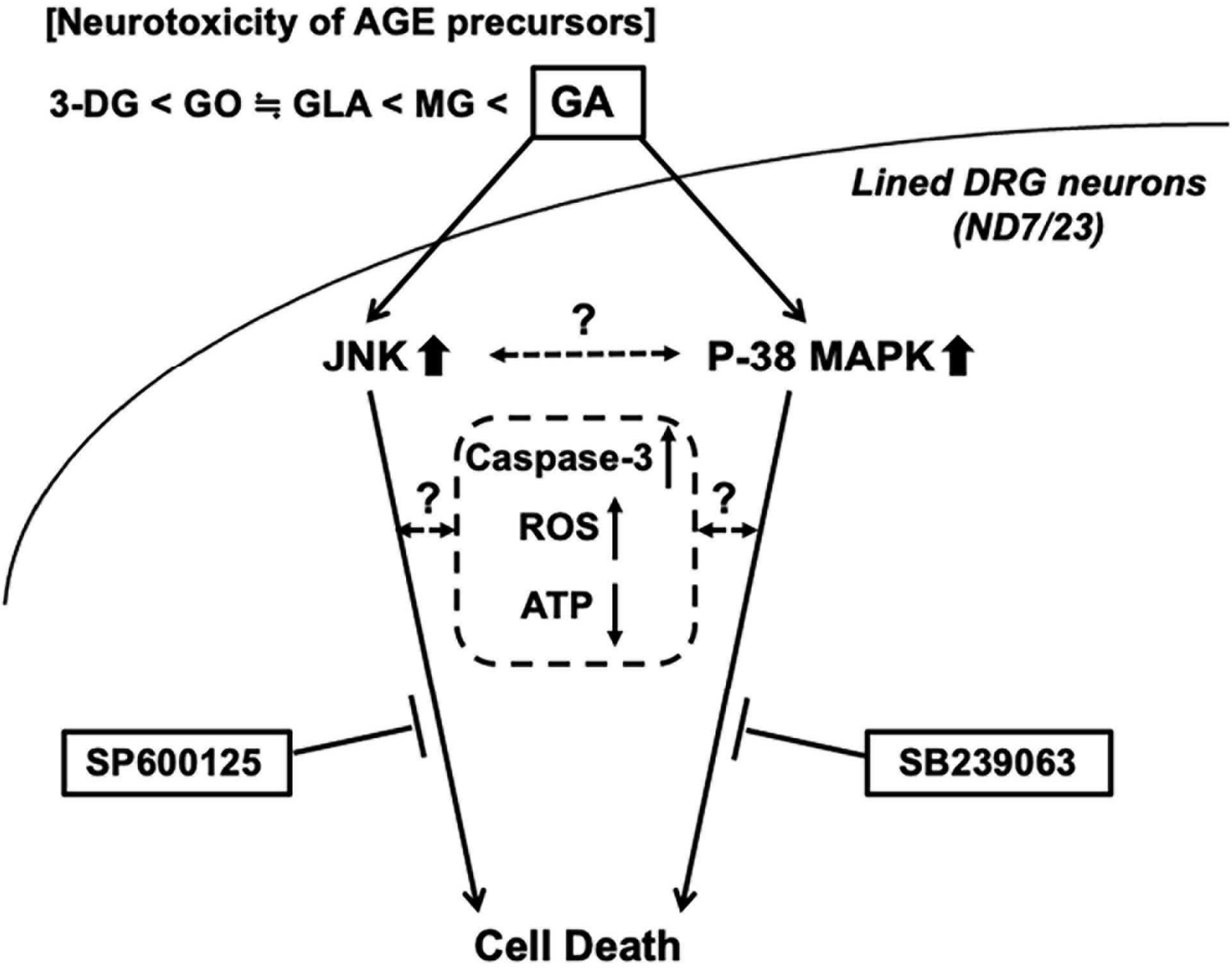
[Neurotoxicity of AGE precursors]
3-DG < GO ≒ GLA < MG < GA
Lined DRG neurons
(ND7/23)
JNK
?
P-38 MAPK
Caspase-3
ROS
ATP
?
?
SP600125
SB239063
Cell Death